The Journal of Veterinary Medical Science

FULL PAPER

Anatomy

Three-dimensional structural analysis of mitochondria composing each subtype of fast-twitch muscle fibers in chicken

Sachi MAKIDA[1)], Kiyokazu KAMETANI[1)], Marina HOSOTANI[1)], Naoki TAKAHASHI[2)], Tomohito IWASAKI[3)], Yasuhiro HASEGAWA[3)], Tomohide TAKAYA[4)], Hiromi UEDA[1)] and Takafumi WATANABE[1)]*

[1)]Department of Veterinary Anatomy, School of Veterinary Medicine, Rakuno Gakuen University, Hokkaido, Japan
[2)]Department of Veterinary Anatomy, College of Bioresource Sciences, Nihon University, Kanagawa, Japan
[3)]Department of Food Science and Human Wellness, College of Agriculture, Food and Environment Science, Rakuno Gakuen University, Hokkaido, Japan
[4)]Department of Agricultural and Life Sciences, Faculty of Agriculture, Shinshu University, Nagano, Japan

ABSTRACT. In a previous study, the three-dimensional structures of mitochondria in type I and type IIb muscle fibers of chicken were analyzed. The study reported differences in the shape of the mitochondria and the distribution of lipid droplets. In this study, we three-dimensionally analyzed mitochondria and lipid droplets of type II muscle fiber subtypes IIa, IIb, and IIc of chicken lateral iliotibial muscle in the same field of view using correlative light electron microscopy (CLEM) and array tomography methods. The reconstructed images showed that the mitochondria of type IIa muscle fiber were thick and aligned along the myofibrils, and many lipid droplets were embedded in the mitochondria. The mitochondria of type IIb muscle fibers were intermittent, aligned along the myofibrils, and showed contact between adjacent horizontal mitochondria. No lipid droplets were observed in type IIb muscle fiber. In type IIc muscle fiber, we observed irregularly shaped mitochondria with small diameters aligned along the myofibrils. Lipid droplets not only were embedded in the mitochondria but also existed independently in some cases. The combination of array tomography and CLEM methods enabled three-dimensional electron microscopic observation of mitochondria in different subtypes of type II muscle fibers. The subtypes of type II muscle fibers differed in mitochondrial occupancy and morphology and in lipid droplet distribution, and characteristics that had been demonstrated biochemically were also demonstrated ultrastructurally.

KEYWORDS: array tomography, correlative light electron microscopy, electron microscopy, fast skeletal muscle, mitochondria

J. Vet. Med. Sci.
84(6): 809–816, 2022
doi: 10.1292/jvms.22-0080

Received: 25 February 2022
Accepted: 1 April 2022
Advanced Epub:
14 April 2022

In general, mammalian skeletal muscle fibers are classified into type I and type II, and subtypes are classified according to the difference in myosin heavy chain isoforms. Mammalian type II muscle fibers include type IIa, type IIb, and type IIx. Type IIa muscle fibers undergo aerobic metabolism, and type IIb muscle fibers undergo anaerobic metabolism. Type IIx has a fatigue tolerance intermediate between type IIa and type IIb muscle fibers [5, 20]. In the past, myosin ATPase histochemistry was used as a method for histological classification of skeletal muscle fiber subtypes, but the process is complicated [6]. In recent years, immunohistochemistry using primary antibodies against the myosin heavy chain has become common as a more accurate and simpler classification method [19].

The subtypes of chicken skeletal muscle fibers are classified as type I, type IIa, type IIb, type IIc, and tonic type, depending on the myosin heavy chain isoform. The function of type IIc muscle fibers is unknown [17]. In a previous study, three-dimensional (3D) electron microscopic analysis of the mitochondria of chicken type I muscle fibers of gastrocnemius muscle and type IIb muscle fibers of pectoralis major muscle was reported [9]. In type I muscle fibers, large mitochondria were present in dense succession and lipid droplets were incorporated into the mitochondria, whereas in type IIb muscle fibers, small mitochondria were

*Correspondence to: Watanabe, T.: t-watanabe@rakuno.ac.jp, Department of Veterinary Anatomy, School of Veterinary Medicine, Rakuno Gakuen University, Midorimachi 582, Bunkyodai, Ebetsu, Hokkaido 069-8501, Japan
(Supplementary material: refer to PMC https://www.ncbi.nlm.nih.gov/pmc/journals/2350/)

present sparsely and lipid droplets were absent, revealing a difference in the 3D ultrastructure [9].

In previous studies using the gastrocnemius muscle, which contains many type I muscle fibers with characteristic ultramicroscopic morphology, and the pectoralis major muscle, which consists only of type IIb muscle fibers, it was easy to identify the muscle fiber subtype under electron microscopy. However, it is difficult to identify each muscle fiber subtype in skeletal muscle, which is composed of hybrids of various type II muscle fibers [19], under electron microscopy. To overcome this problem, in the present study, the 3D structure of mitochondria in type II muscle fibers was analyzed using the correlative light electron microscopy (CLEM) method [15] and the array tomography method [12]. The subtypes of type II muscle fibers were identified using immunohistochemistry with primary antibodies that can differentially stain the respective subtypes of type II muscle fibers, and the 3D structure of the mitochondria of each muscle fiber was analyzed under electron microscopy in the same field of view using the array tomography method.

MATERIALS AND METHODS

Experimental animals

The animal experiments in this study were approved by the Institutional Animal Care and Use Committee of Rakuno Gakuen University (Approval No.: VH20A11), in accordance with the Act on Welfare and Management of Animals of the Japanese Government. Two broiler chickens (ROSS 308, male), 47 and 97 days-of-age respectively, raised on the university farm, were euthanized by exsanguination under deep anesthesia by intravenous injection of 20–30 mg/kg pentobarbital sodium (Somnopentyl; Kyoritsu Pharmaceutical Co., Tokyo, Japan).

CLEM method

The lateral iliotibial muscle, which consists only of type IIa, IIb, and IIc muscle fibers, from the 97-day-old chicken was cut into 10 × 10 × 10 mm pieces along the long axis [14]. After the samples were cut out, they were immersion-fixed in 0.5% glutaraldehyde + 0.5% paraformaldehyde/0.1 M phosphate buffer solution at 4°C. After fixation, the samples were immersed in 10%, 20%, and 30% sucrose solution at 4°C for 1 day each, embedded in optimal cutting temperature compound (Sakura Finetek Japan Co., Ltd., Tokyo, Japan), and frozen at −80°C. Serial sections of 10-µm thickness were prepared from the frozen samples using a cryostat, and immunohistochemistry and transmission electron microscopy (TEM) were performed in accordance with the following procedures.

Immunohistochemistry: The primary antibody used was a mouse anti-fast muscle antibody (M4276; Sigma Aldrich Co., LLC., St. Louis, MO, USA), which can be used to identify subtypes of chicken type II muscle fibers according to the staining intensity (Supplementary Data 1).

Frozen sections were washed with 0.05 M phosphate-buffered saline (PBS; pH 7.4), immersed in antigen activation solution (HistoVT One; Nacalai Tesque, Kyoto, Japan) and heated at 70°C for 20 min. The sections were then washed with PBS and treated with 0.3% H_2O_2 methanol for 20 min at room temperature to remove endogenous peroxidase. The sections were pretreated with blocking agent (Blocking One Histo; Nacalai Tesque) for 10 min at room temperature and washed with 0.1% Triton X-loaded PBS for 5 min. The sections were incubated with mouse anti-fast muscle antibody diluted 1:10,000 with immunoreactivity sensitizing reagent (Can Get Singal; TOYOBO, Osaka, Japan) overnight at 4°C. After being washed with PBS, the sections were incubated with rabbit biotinylated anti-mouse IgG + IgA + IgM antibody (HISTOFINE; Nichirei Bioscience Inc., Tokyo, Japan) for 30 min and with horseradish peroxidase-conjugated streptavidin (diluted 1:300; SP20C, Stereospecific Detection Technologies, Baesweiler, Germany) for 30 min at room temperature. The sections were washed with PBS three times for 5 min after each incubation step. Immunocomplexes were visualized with 0.05% 3,3′-diaminobenzidine solution in Tris-HCl buffer (pH 7.4) for 4 min. Sections subjected to immunohistochemistry were observed under a light microscope; the field of view where type IIa, type IIb, and type IIc muscle fibers were present was observed and images were taken.

TEM: Frozen sections that were not subjected to immunohistochemistry were immersed in PBS followed by immersion in 0.1 M cacodylate buffer (pH 7.4). Sections were immersed in 2.5% glutaraldehyde/0.1 M cacodylate buffer for 10 min at room temperature, followed by washing in 0.1 M cacodylate buffer for 10 min at room temperature and then washing with 0.1 M cacodylate buffer four times (4 min each). Then, they were immersed in 2% OsO_4 (TAAB Laboratories Equipment Ltd., Berks, UK) in 1.5% potassium ferrocyanide trihydrate (Nacalai Tesque) in 0.1 M cacodylate buffer for 30 min on ice. The samples were then washed with distilled water four times (4 min each), immersed in 1% thiocarbohydrazide (Sigma Aldrich) for 10 min at room temperature, and washed with distilled water four times (4 min each). Then, they were immersed in 2% OsO_4 for 15 min at room temperature and washed with distilled water four times (4 min each), then immersed in 1% uranium acetate solution at 4°C overnight. The samples were washed with distilled water four times (4 min each), and immersed in Walton's lead aspartate solution for 30 min at 60°C. The samples were dehydrated with an ethanol gradient series, transferred to QY-1, and finally embedded in epoxy resin (Quetol 812; Nissin EM, Tokyo, Japan) [21].

The area of the resin-embedded block containing muscle fibers identical to those observed by immunohistochemistry was trimmed to 1 × 1 mm and sliced to 120-nm thickness using an ultramicrotome (EM UC7; Leica, Wetzler, Germany). Ultrathin sections were placed on a single-hole grid with a Holmbar support membrane and mounted on a transmission electron microscope (HT-7700; Hitachi High-Technologies Corp., Tokyo, Japan) for observation and image capture at an acceleration voltage of 80 kV.

Ten images of each subtype of type II muscle fiber, which were identified by matching with the information in the light microscope (immunohistochemistry) images, were taken at ×2,000 magnification (792.085 µm^2 squares). The area of a

mitochondrion, the number of mitochondria, and the percentage of the total area occupied by mitochondria in muscle fiber in each image were determined using image analysis software (Image Pro Premier; Roper Japan, Tokyo, Japan). The area of a lipid droplet, the number of lipid droplets, and the percentage of the total area occupied by lipid droplets were also determined.

Array tomography

The lateral iliotibial muscle from the 47-day-old chicken was cut into 1 × 1 ×10 mm sections along the long axis. The samples were immersed and fixed in half Karnofsky solution (2.5% glutaraldehyde + 2% paraformaldehyde/0.1 M cacodylate solution, pH 7.4) overnight at 4°C. Epon resin embedding was performed by the same process as described above for embedding for TEM, however, the immersion time in each reagent was modified: Briefly, the samples were immersed in 2% OsO_4 in 1.5% potassium ferrocyanide trihydrate for 1 hr on ice, 1% thiocarbohydrazide for 20 min, 2% OsO_4 for 30 min, and Walton's lead aspartate solution for 1 hr at 60°C.

The resin-embedded samples were trimmed to 1 × 1 mm and ultrathin sections (120-nm) were cut perpendicular to the long axis of the muscle fiber. Forty-nine ultrathin sections were prepared in succession, placed on a silicon wafer and coated with 10 nm osmium. The silicon wafers were mounted on aluminum stubs using conductive adhesive. Forty-nine consecutive images were acquired using a scanning electron microscope (SEM; JSM-IT800; JEOL, Tokyo, Japan) at an acceleration voltage of 7 kV for 3D imaging. Using image analysis software (Image Pro Premier), the image of region containing type II muscle fibers of all subtypes, classified according to the characteristics of the respective mitochondria identified in the CLEM experiments, was trimmed to 40 µm square per side.

Three-dimensional images of the mitochondria and lipid droplets in each muscle fiber type were reconstructed. For an object to qualify as a mitochondrion, at least one of the lipid bilayers and cristae structure must be identifiable; for lipid droplets, four or more consecutive circular pieces of uniformly electron-dense material could be identified. From the obtained 3D images of each muscle fiber type, the volume of a mitochondrion, the number of mitochondria, and the percentage of mitochondrial volume in the muscle fiber were determined using image analysis software (Image Pro Premier) according to a previous method [9]. The volume of a lipid droplet, the number of lipid droplets, and the percentage lipid droplet volume were also determined.

Statistical analysis

Results are expressed as the mean ± standard deviation (SD); data for two groups were compared using Student's *t*-test ($P<0.01$), and data for three groups were compared using Tukey-Kramer's test ($P<0.05$, $P<0.01$).

RESULTS

CLEM

In immunohistochemistry, the muscle fibers of the lateral tibialis muscle of chicken exhibited three types of staining, identified as type IIa, type IIb, and type IIc muscle fibers, respectively. The distribution of muscle fibers of each subtype in the observed visual field was dominated by type IIb muscle fibers, and type IIa and type IIc muscle fibers were distributed in similar proportions. The diameter of type IIa muscle fibers was small, and that of type IIb muscle fibers was large. The diameter of type IIc muscle fibers varied from small to large (Fig. 1).

By combining the immunohistochemistry images (Fig. 2a) and TEM images (Fig. 2b) prepared from frozen serial sections, we were able to identify the muscle fiber subtypes in TEM observations (Fig. 2c). TEM observations showed features of the mitochondria of each subtype of type II muscle fiber (Fig. 3). Mitochondria and lipid droplets were present between the myofibrils and varied in size, shape, and occupancy. Mitochondria in type IIa muscle fibers were large (0.274 ± 0.17 µm^2) and densely packed (1.93 ± 0.37%). Mitochondria in type IIb muscle fibers were small (0.265 ± 0.15 µm^2) and sparsely distributed (1.16 ± 0.31%). Mitochondria in type IIc muscle fibers were small (0.248 ± 0.13 µm^2) and sparsely distributed (1.19 ± 0.32%). Statistical analysis showed that the two-dimensional area of a mitochondrion in type IIa muscle fibers was significantly larger than that in type

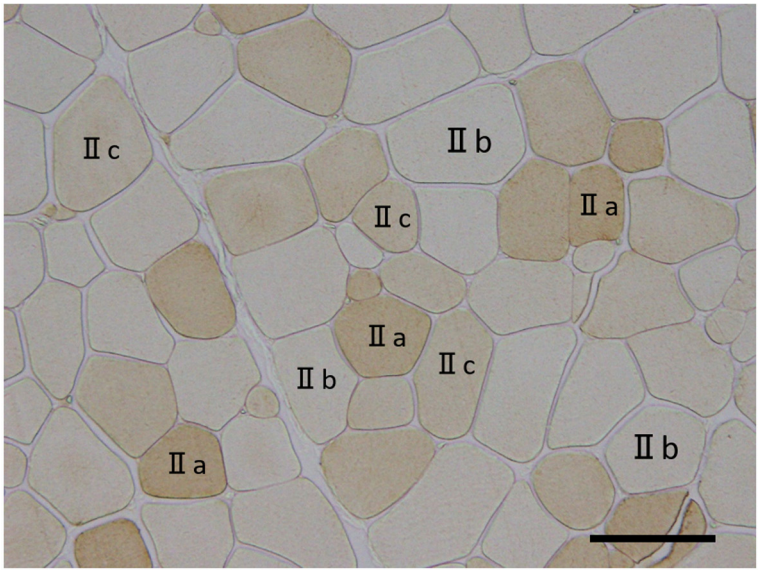

Fig. 1. Immunohistochemical staining of fast-twitch muscle fibers in chicken lateral iliotibial muscle. Image of area where muscle fibers of each subtype are in close proximity. Strongly positive-staining muscle fibers are type IIa, negative-staining muscle fibers are type IIb, and weakly positive-staining muscle fibers are type IIc. Type IIa muscle fibers have a smaller diameter than type IIb fibers. Bar=100 µm.

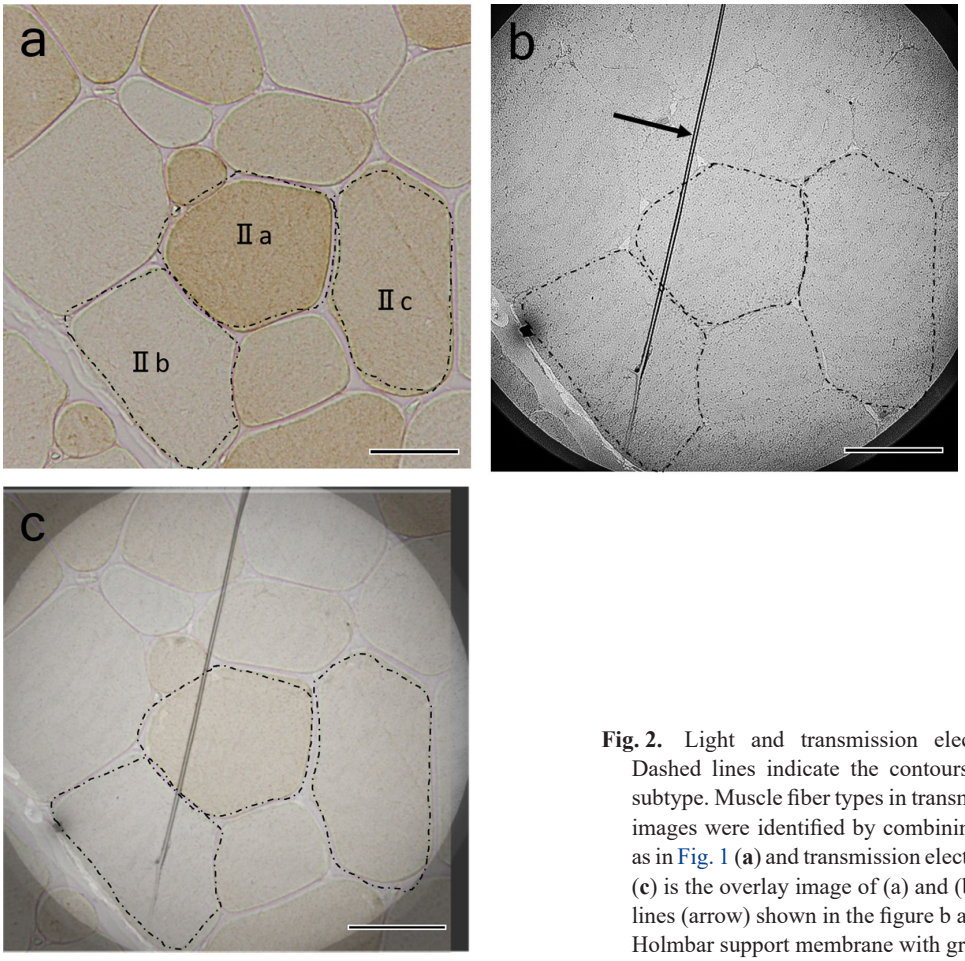

Fig. 2. Light and transmission electron microscopy images. Dashed lines indicate the contours of muscle fibers of each subtype. Muscle fiber types in transmission electron microscopy images were identified by combining light microscopy images as in Fig. 1 (**a**) and transmission electron microscopy images (**b**); (**c**) is the overlay image of (a) and (b). The two vertical oblique lines (arrow) shown in the figure b are wrinkles, artifacts, of the Holmbar support membrane with grid. Bars=50 µm.

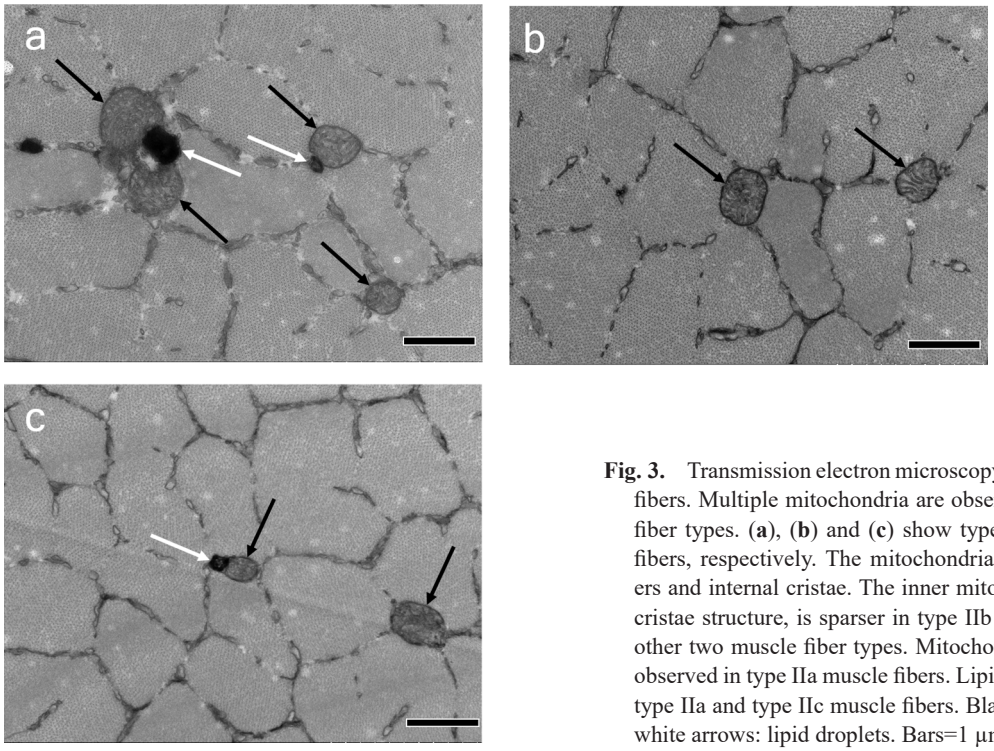

Fig. 3. Transmission electron microscopy images of type II muscle fibers. Multiple mitochondria are observed in all type II muscle fiber types. (**a**), (**b**) and (**c**) show type IIa, IIb, and IIc muscle fibers, respectively. The mitochondria also contain lipid bilayers and internal cristae. The inner mitochondrial membrane, the cristae structure, is sparser in type IIb muscle fibers than in the other two muscle fiber types. Mitochondria are most frequently observed in type IIa muscle fibers. Lipid droplets are observed in type IIa and type IIc muscle fibers. Black arrows: mitochondria; white arrows: lipid droplets. Bars=1 µm.

IIc muscle fibers. The number of mitochondria per unit area and the mitochondrial density as a percentage of the area were significantly greater in type IIa muscle fibers than in type IIb and type IIc muscle fibers (Table 1). Lipid droplets were observed in type IIa and type IIc muscle fibers. The two-dimensional area of lipid droplets of type IIa and type IIc were 0.083 ± 0.10 μm^2 and 0.036 ± 0.02 μm^2, respectively, and significantly larger in type IIa muscle fibers than in type IIc muscle fibers, but there was no significant difference in the number of lipid droplets or the percentage area occupied by lipid droplets per field of view (Table 2).

Array tomography

Three-dimensional reconstructed images of mitochondria of type IIa, IIb, and IIc muscle fibers could be observed in the same field of view (Fig. 4a–c and Supplementary Movie 1). In the 3D imaging, the volume of mitochondria was significantly larger in type IIa than in type IIb and IIc fibers. The number of mitochondria per unit volume was highest for type IIb. The distribution density was highest in type IIa muscle fibers (Table 3). No significant difference in the volume of lipid droplets was observed between type IIa and type IIc fibers (Table 4).

Columnar mitochondria were observed in type IIa and type IIc fibers. Columnar mitochondria were thicker and more abundant between myofibrils in type IIa fibers than in type IIc fibers (Fig. 4a–c). In type IIb fibers, mitochondria were linearly arranged along the myofibrils, but their diameters were different in some places (Fig. 4b).

Observation of type IIa muscle fibers: In type IIa myofibrils, mitochondria aligned linearly along the myofibrils and small mitochondria scattered throughout the myofibrils were observed. The mitochondria aligned linearly with the myofibrils were often embedded with lipid droplets (Fig. 5a).

Observation of type IIb muscle fibers: In type IIb myofibrils, mitochondria with small diameters aligned along the myofibrils and mitochondria that were aligned but spatially separated were observed. Mitochondria in contact with neighboring mitochondria were also observed. No lipid droplets were observed (Fig. 5b).

Table 1. The area of a mitochondrion, the number of mitochondria, and the percentage area occupied by mitochondria in muscle fiber measured from transmission electron microscopic images

	Mitochondrion area (μm^2)	Mitochondrion number (number/1,000 μm^2)	Mitochondrial area in the muscle fibers (%)
Type IIa	0.274 ± 0.17	68.9 ± 4.5	1.93 ± 0.37
Type IIb	0.265 ± 0.15	43.7 ± 8.6**	1.16 ± 0.31**
Type IIc	0.248 ± 0.13*	48.4 ± 16.2**	1.19 ± 0.32**

Compared with type IIa muscle fibers, *P<0.05, **P<0.01. The number of mitochondria per unit area is calibrated per 1,000 μm^2.

Table 2. The area of a lipid droplet, the number of lipid droplets, and the percentage area occupied by lipid droplets in muscle fiber measured from transmission electron microscopic images of type IIa and IIc muscle fibers

	Lipid droplet area (μm^2)	Lipid droplets number (number/1,000 μm^2)	Lipid droplet area in the muscle fibers (%)
Type IIa	0.083 ± 0.10	3.9 ± 1.4	0.033 ± 0.030
Type IIc	0.036 ± 0.02*	3.7 ± 2.0	0.013 ± 0.009

Compared with type IIa muscle fibers, *P<0.05. The number of lipid droplets per unit area is calibrated per 1,000 μm^2.

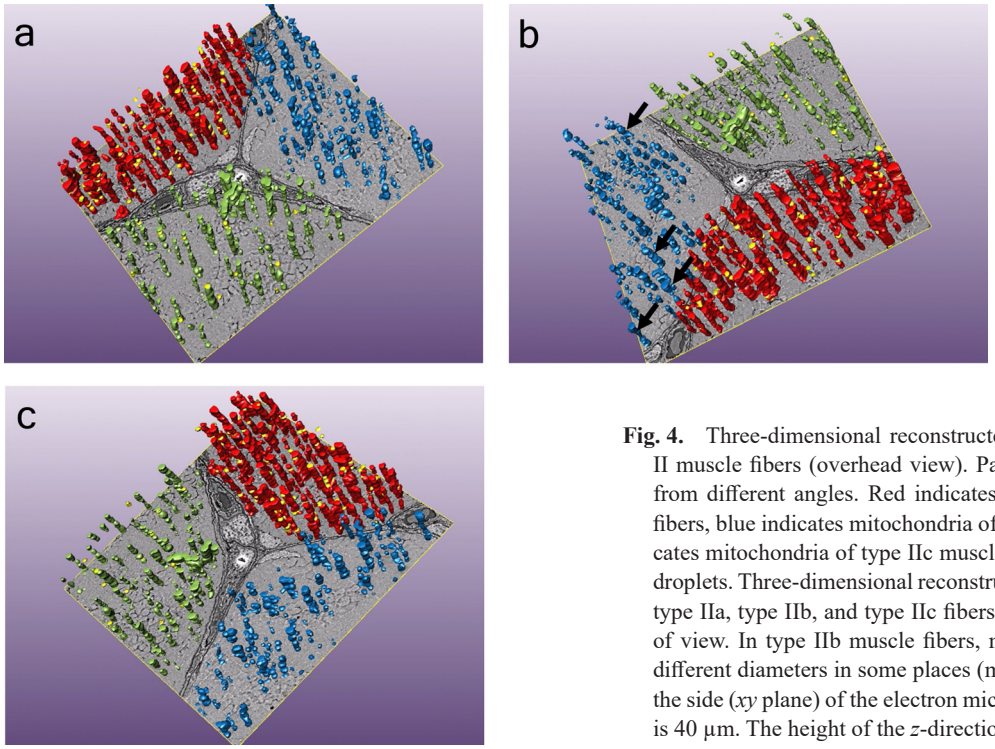

Fig. 4. Three-dimensional reconstructed image of mitochondria in type II muscle fibers (overhead view). Panels (**a**–**c**) show the whole image from different angles. Red indicates mitochondria of type IIa muscle fibers, blue indicates mitochondria of type IIb muscle fibers, green indicates mitochondria of type IIc muscle fibers, and yellow indicates lipid droplets. Three-dimensional reconstructed images of mitochondria from type IIa, type IIb, and type IIc fibers can be observed in the same field of view. In type IIb muscle fibers, mitochondria are aligned but have different diameters in some places (marked with arrows). The length of the side (*xy* plane) of the electron micrograph at the bottom in figure a–c is 40 μm. The height of the *z*-direction is 5.88 μm.

Table 3. The volume of a mitochondrion, the number of mitochondria, and the percentage volume occupied by mitochondria in muscle fibers measured from 3D images

	Mitochondrion volume (μm^3)	Mitochondrion number (number/ μm^3)	Mitochondrial volume in the muscle fibers (%)
Type IIa	2.01 ± 2.64	0.046	9.29
Type IIb	0.41 ± 0.64**	0.066	2.69
Type IIc	0.70 ± 1.24**	0.043	3.04

Compared with type IIa muscle fibers, $^{**}P<0.01$.

Table 4. The volume of a lipid droplet, the number of lipid droplets, and the percentage volume occupied by lipid droplets in muscle fibers measured from 3D images of type IIa and IIc muscle fibers

	Lipid droplet volume (μm^3)	Lipid droplets number (number/ μm^3)	Lipid droplets volume in the muscle fibers (%)
Type IIa	0.15 ± 0.11	0.032	0.46
Type IIc	0.13 ± 0.06	0.005	0.06

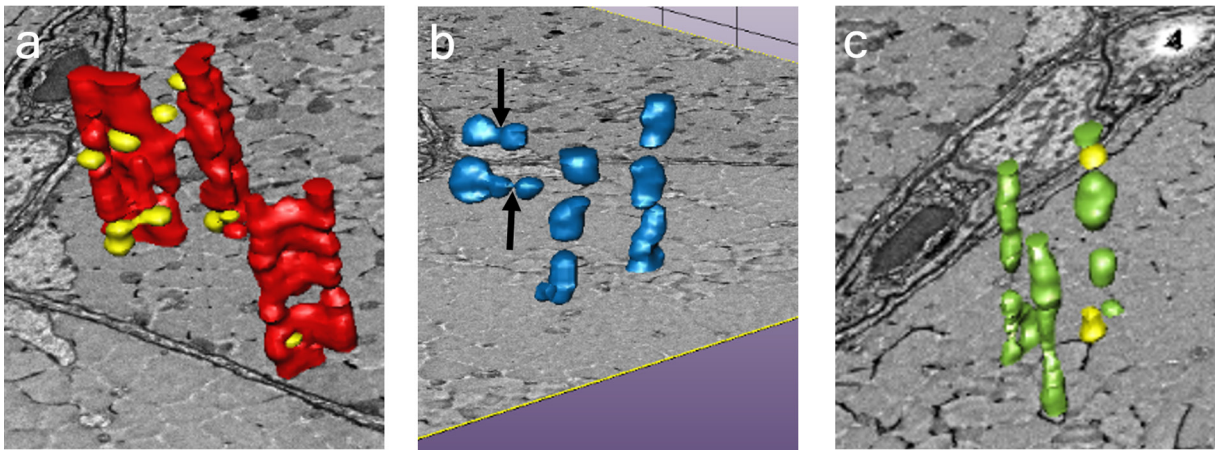

Fig. 5. Magnified images of three-dimensional reconstructions of mitochondria from each muscle fiber subtype. (**a**) Linear mitochondria with embedded lipid droplets (yellow) are observed in type IIa muscle fibers. (**b**) Many isolated mitochondria are observed, but some mitochondria are associated with adjacent mitochondria (marked with arrows) in type IIb muscle fibers. (**c**) Both continuous and isolated mitochondria are observed, and lipid droplets are also present, in type IIc muscle fibers.

Observation of type IIc muscle fibers: In type IIc myofibrils, relatively thin mitochondria aligned linearly along the myofibrils and separated mitochondria aligned linearly along the myofibrils were observed. Lipid droplets were also observed; some were embedded in mitochondria as in type IIa myofibrils, but some lipid droplets were independent of mitochondria (Fig. 5c).

DISCUSSION

To our knowledge, this is the first report of 3D structural reconstruction of mitochondria of different subtypes of muscle fibers in the same field of view.

According to the results of immunohistochemistry, the distribution of muscle fibers of each subtype in the observed visual field was dominated by type IIb muscle fibers, and type IIa and type IIc muscle fibers were distributed in similar proportions. This is consistent with the muscle fiber type distribution of the lateral iliotibial muscle revealed by Roy *et al*. using histochemical classification methods [14]. Although there are methods of tissue staining for each subtype of muscle fiber [19], no reports have combined light (staining) and electron microscopy images. In the present study, the CLEM method enabled us to analyze the ultrastructural features of mitochondria of all type II muscle fiber subtypes in the same field of view.

The serial block face (SBF)-SEM method [15] was used to analyze chicken type I and type IIb muscle fibers in a previous study [9]. This is a method that can automatically acquire hundreds of serial sections at 50-nm thickness intervals in the *z*-direction. However, the SBF-SEM method has a narrow field of view in the *xy* plane and it is difficult to use in combination with the CLEM method, making it unsuitable for acquiring serial ultrathin sections of multiple muscle fiber subtypes in the same area as we have done in the present study.

The array tomography method used in this study has the disadvantage that the *z*-pitch is thicker and the shape of the 3D reconstructed images is rougher than those from the SBF-SEM method because continuous sections are acquired at 120-nm thickness intervals. However, the advantage of the array tomography method is that it allows us to observe a wide area as many times as we want, so we can compare muscle fiber subtypes in the same field of view. In addition, the concern that the thicker *z*-pitch may cause continuous construction of mitochondria that are in reality separate was resolved by constructing many mitochondria in a large volume. Therefore, the combination of CLEM and array tomography methods used in this study was valuable for 3D reconstruction of the mitochondria in each muscle fiber subtype.

Three-dimensional reconstructed electron microscopy images of mitochondria of fast and slow-twitch muscles in mice and type I and type II muscle fibers in humans have been reported [4, 7]. However, no report classifies skeletal muscle fibers in mammalian by subtype, such as type IIa and type IIb, and analyses each 3D structure of mitochondria. Three-dimensional reconstructed images of the mitochondria of type I and type IIb muscle fibers have been reported in studies on chicken, and it is clear that the morphology of each is different [9]. The morphology of the mitochondria of type IIb muscle fibers of the chicken pectoralis major muscle in previous study [9] and the mitochondria of type IIb muscle fibers of the lateral iliotibial muscle in the present study were similar. These results indicate that the features of the 3D reconstructed images of muscle fiber subtypes are maintained in different individuals and skeletal muscles, at least in chickens. In addition, the present 3D mitochondrial analysis method by subtypes would offer applications to the study of muscle fibers in other animals, not only in physiological conditions but also in aging and injured states.

Our previous study has reported that the 2D mitochondrial observations could not show the substantial mitochondrial size, shape, and network frame among the myofibers, and the percentage of mitochondria in muscle fibers under electron microscopic analysis is higher in 3D measurements than in 2D, which this was also verified in the present subtype analysis of different fast-twitch muscles (Tables 1 and 3) [9]. As shown in Tables 2 and 4, the density of lipid droplets in the planar and 3D images also differed between type IIa and type IIc muscle fibers. The reason for this may be that lipid droplets are more abundant in mitochondria that have a tubular network. Dahl *et al*. in their 3D analysis of mitochondria in human type I and type II muscle fibers reported that mitochondrial lipid droplets are regularly located along the Z line (I band) of myofibrils [4]. Therefore, it is considered that differences in the transverse area and density of lipid droplets occur due to delicate differences in the angle of transverse sectioning when ultrathin sections are made perpendicular to the long axis of myofibrils in two-dimensional TEM observation and whether or not the ultrathin section includes the I band. Therefore, the present 3D analysis method is useful for understanding the morphology and distribution not only of type IIa and type IIc mitochondria but also of lipid droplets.

The 3D properties of the mitochondria in the different subtypes of muscle fiber correspond to physiological phenotypes specific to the muscle fiber type. Mitochondrial content has been considered to correlate with oxidative capacity, muscle fiber contractility, and mitochondrial interrelationships with metabolic activity status [4, 9, 22]. Type IIa muscle fibers undergo aerobic metabolism [2]. The thick and continuous mitochondria and the 3D structure of lipid droplets regularly incorporated into the mitochondria (Fig. 4) elucidated in this study proved that type IIa muscle fibers have structural characteristics suitable for aerobic metabolism [9]. This feature was also similar to that of type I muscle fibers observed in a previous study [9]. However, the diameter of the mitochondria in type IIa myofibrils was lower than of those in type I myofibrils, they were less dense, and the proportion of myofibrils was higher. Lipid droplets were smaller and fewer in number than in type I muscle fibers [9]. This information indicated that type IIa muscle fibers had stronger contractility than type I muscle fibers, although the muscle fibers were classified as having the same aerobic metabolism.

Similarly, type IIb muscle fibers, which contain isolated mitochondria and lack lipid droplets, were ultrastructurally shown to contribute to anaerobic metabolism (Fig. 4) [20]. The contacts with adjacent mitochondria observed in type IIb myofibrils are thought to be fission or fusion (in general, mitochondria are dynamic organelles that undergo repeated fission and fusion) [4]. Mitochondria in type IIb muscle fibers are not always isolated, but may be in a discontinuous network with surrounding mitochondria. Differences in gene expression between fusion and fission may regulate the differences in mitochondrial morphology of each subtype, which would be revealed by gene expression analysis in in-situ quantification of each subtype. This expectation would also be mentioned regarding genes related to the morphology of lipid droplets. For example, Perilipin 5, known as lipid droplet-associated protein, is one of the proteins that mediate between mitochondria and lipid droplets [8]. It has been reported that the protein content of Perilipin 5 correlated with OXPHOS content and with mitochondrial respiration rates on a lipid-derived substance [3]. Although it was unable to analyze the expression levels of lipid-associated proteins for each muscle fiber subtype in the present study, differences in such protein expression suggest that they affect lipid droplet size and mitochondrial contact between different muscle subtypes.

One study has reported that the NADH dehydrogenase activity of chicken type IIc muscle fibers is intermediate between that of type IIa and type IIb fibers, but it was unclear whether the type IIc muscle fibers exhibit aerobic or anaerobic metabolism [17]. The 3D reconstructed image of the mitochondria of type IIc muscle fibers in this study has both type IIa and type IIb characteristics, suggesting that they are intermediate between aerobic metabolism type IIa and anaerobic metabolism type IIb. The existence of type IIx, but not type IIc, muscle fibers have been reported in mammals. Type IIx muscle fiber has been reported to have characteristics intermediate between mammalian type IIa and type IIb by biochemical analysis [20]. On the basis of this information and the results of the present study, we suggest that the muscle fibers previously classified as type IIc in chicken correspond to mammalian type IIx muscle fibers.

In mammals, muscle fiber type switching is caused by nerve activity, denervation, and long-term paralysis [11, 16, 18, 19]. Other external factors, such as load changes and external electrical stimulation, can also cause muscle fiber type switching [1, 12, 13, 19], and endocrine disorders, such as thyroid dysfunction, can also be a factor [10]. The present ultrastructural analysis of chicken type IIc muscle fibers showed that they have properties intermediate between type IIa and type IIb fibers, and the diameter of the muscle fibers was uneven in the light microscope images, suggesting that they may be muscle fibers that differentiate into type IIa and type IIb due to factors such as those described above.

In chickens, in addition to type I and type II muscle fiber subtypes, the existence of tonic type muscle fibers has been reported [17]. Tonic type muscle fibers, such as type IIc muscle fibers, are classified as muscle fibers of unknown function in chickens. The tonic type is distributed in the adductor profound muscle and has similar properties to type I muscle fibers, indicating that the type

IIc muscle fibers observed in this study have ultrastructural features that are clearly different from those of the tonic type [14, 17].

This study showed that chicken skeletal muscle fiber types can be classified by the characteristic 3D structures of their mitochondria, which may be a new indicator for skeletal muscle fiber type classification.

CONFLICT OF INTEREST. The authors declare no conflict of interest.

ACKNOWLEDGMENTS. The authors thank JEOL Ltd. for technical support with an SEM analysis. This work was supported by Grant-in-Aid Scientific Research (C) from Japan Society for the Promotion Science (No. 21K05942 to T.W.), and Rakuno Gakuen University Research Fund (No. 2021-4 to T.W.).

REFERENCES

1. Ausoni, S., Gorza, L., Schiaffino, S., Gundersen, K. and Lømo, T. 1990. Expression of myosin heavy chain isoforms in stimulated fast and slow rat muscles. *J. Neurosci.* **10**: 153–160. [Medline] [CrossRef]
2. Benador, I. Y., Veliova, M., Liesa, M. and Shirihai, O. S. 2019. Mitochondria bound to lipid droplets: where mitochondrial dynamics regulate lipid storage and Utilization. *Cell Metab.* **29**: 827–835. [Medline] [CrossRef]
3. Bosma, M., Minnaard, R., Sparks, L. M., Schaart, G., Losen, M., de Baets, M. H., Duimel, H., Kersten, S., Bickel, P. E., Schrauwen, P. and Hesselink, M. K. C. 2012. The lipid droplet coat protein perilipin 5 also localizes to muscle mitochondria. *Histochem. Cell Biol.* **137**: 205–216. [Medline] [CrossRef]
4. Dahl, R., Larsen, S., Dohlmann, T. L., Qvortrup, K., Helge, J. W., Dela, F. and Prats, C. 2015. Three-dimensional reconstruction of the human skeletal muscle mitochondrial network as a tool to assess mitochondrial content and structural organization. *Acta Physiol. (Oxf.)* **213**: 145–155. [Medline] [CrossRef]
5. DeNardi, C., Ausoni, S., Moretti, P., Gorza, L., Velleca, M., Buckingham, M. and Schiaffino, S. 1993. Type 2X-myosin heavy chain is coded by a muscle fiber type-specific and developmentally regulated gene. *J. Cell Biol.* **123**: 823–835. [Medline] [CrossRef]
6. Engel, W. K. 2015. Diagnostic histochemistry and clinical-pathological testings as molecular pathways to pathogenesis and treatment of the ageing neuromuscular system: a personal view. *Biochim. Biophys. Acta* **1852**: 563–584. [Medline] [CrossRef]
7. Glancy, B., Hartnell, L. M., Malide, D., Yu, Z. X., Combs, C. A., Connelly, P. S., Subramaniam, S. and Balaban, R. S. 2015. Mitochondrial reticulum for cellular energy distribution in muscle. *Nature* **523**: 617–620. [Medline] [CrossRef]
8. Henne, W. M., Reese, M. L. and Goodman, J. M. 2018. The assembly of lipid droplets and their roles in challenged cells. *EMBO J.* **37**: e98947. [Medline] [CrossRef]
9. Hosotani, M., Kametani, K., Ohno, N., Hiramatsu, K., Kawasaki, T., Hasegawa, Y., Iwasaki, T. and Watanabe, T. 2021. The unique physiological features of the broiler pectoralis major muscle as suggested by the three-dimensional ultrastructural study of mitochondria in type IIb muscle fibers. *J. Vet. Med. Sci.* **83**: 1764–1771. [Medline] [CrossRef]
10. Izumo, S., Nadal-Ginard, B. and Mahdavi, V. 1986. All members of the MHC multigene family respond to thyroid hormone in a highly tissue-specific manner. *Science* **231**: 597–600. [Medline] [CrossRef]
11. Jerkovic, R., Argentini, C., Serrano-Sanchez, A., Cordonnier, C. and Schiaffino, S. 1997. Early myosin switching induced by nerve activity in regenerating slow skeletal muscle. *Cell Struct. Funct.* **22**: 147–153. [Medline] [CrossRef]
12. Pette, D. 1998. Training effects on the contractile apparatus. *Acta Physiol. Scand.* **162**: 367–376. [Medline] [CrossRef]
13. Pette, D. and Vrbová, G. 1999. What does chronic electrical stimulation teach us about muscle plasticity? *Muscle Nerve* **22**: 666–677. [Medline] [CrossRef]
14. Roy, B. C., Oshima, I., Miyachi, H., Shiba, N., Nishimura, S., Tabata, S. and Iwamoto, H. 2007. Histochemical properties and collagen architecture of M. iliotibialis lateralis and M. puboischiofemoralis in male broilers with different growth rates induced by feeding at different planes of nutrition. *Br. Poult. Sci.* **48**: 312–322. [Medline] [CrossRef]
15. Saitoh, S., Ohno, N., Saitoh, Y., Terada, N., Shimo, S., Aida, K., Fujii, H., Kobayashi, T. and Ohno, S. 2018. Improved serial sectioning techniques for correlative light-electron microscopy mapping of human langerhans islets. *Acta Histochem. Cytochem.* **51**: 9–20. [Medline] [CrossRef]
16. Salmons, S. and Sréter, F. A. 1976. Significance of impulse activity in the transformation of skeletal muscle type. *Nature* **263**: 30–34. [Medline] [CrossRef]
17. Saneyasu, T., Kimura, S., Kitashiro, A., Tsuchii, N., Tsuchihashi, T., Inui, M., Honda, K. and Kamisoyama, H. 2015. Differential regulation of the expression of lipid metabolism-related genes with skeletal muscle type in growing chickens. *Comp. Biochem. Physiol. B Biochem. Mol. Biol.* **189**: 1–5. [Medline] [CrossRef]
18. Sato, Y., Shimizu, M., Mizunoya, W., Wariishi, H., Tatsumi, R., Buchman, V. L. and Ikeuchi, Y. 2009. Differential expression of sarcoplasmic and myofibrillar proteins of rat soleus muscle during denervation atrophy. *Biosci. Biotechnol. Biochem.* **73**: 1748–1756. [Medline] [CrossRef]
19. Sawano, S., Komiya, Y., Ichitsubo, R., Ohkawa, Y., Nakamura, M., Tatsumi, R., Ikeuchi, Y. and Mizunoya, W. 2016. A one-step Immunostaining method to visualize rodent muscle fiber type within a single specimen. *PLoS One* **11**: e0166080. [Medline] [CrossRef]
20. Schiaffino, S. and Reggiani, C. 2011. Fiber types in mammalian skeletal muscles. *Physiol. Rev.* **91**: 1447–1531. [Medline] [CrossRef]
21. Thai, T. Q., Nguyen, H. B., Saitoh, S., Wu, B., Saitoh, Y., Shimo, S., Elewa, Y. H., Ichii, O., Kon, Y., Takaki, T., Joh, K. and Ohno, N. 2016. Rapid specimen preparation to improve the throughput of electron microscopic volume imaging for three-dimensional analyses of subcellular ultrastructures with serial block-face scanning electron microscopy. *Med. Mol. Morphol.* **49**: 154–162. [Medline] [CrossRef]
22. Wang, Y. and Pessin, J. E. 2013. Mechanisms for fiber-type specificity of skeletal muscle atrophy. *Curr. Opin. Clin. Nutr. Metab. Care* **16**: 243–250. [Medline] [CrossRef]